



## Electrochemical behavior of thionine at titanate nanotubes-based modified electrode: A sensing platform for the detection of trichloroacetic acid

Hong Dai<sup>a</sup>, Huifeng Xu<sup>a</sup>, Xiaoping Wu<sup>a</sup>, Yanyu Lin<sup>a</sup>, Mingdeng Wei<sup>b</sup>, Guonan Chen<sup>a,\*</sup>

<sup>a</sup> Ministry of Education Key Laboratory of Analysis and Detection for Food Safety, Fujian Province Key Laboratory of Analysis and Detection for Food Safety, and Department of Chemistry, Fuzhou University, Fuzhou, Fujian 350002, China

<sup>b</sup> Institute of Energy Technology and Nano-Materials and Department of Chemistry, Fuzhou University, Fuzhou, Fujian 350002, China

### ARTICLE INFO

#### Article history:

Received 22 September 2009

Received in revised form 15 February 2010

Accepted 18 February 2010

Available online 25 February 2010

#### Keywords:

Thionine

Titanate nanotubes

Sensing platform

Trichloroacetic acid

### ABSTRACT

Titanate nanotubes (TNTs) have some unique and seductive properties, such as good biocompatibility, negative charge after treating with weak bases and supply of special reaction vessel for analyte due to their hydroxyls and multilayered structures. Herein, titanate nanotubes were firstly self-assembled on the chitosan (CHIT) membrane modified electrode. Then thionine, as a model electrochemical probe, was firmly immobilized onto the titanate nanotubes (TNTs)-based sensing interface. This strategy provided a new route to immobilize the redox mediator onto the sensing interface. Based on which, trichloroacetic acid (TCA) was found to be able to accelerate the electron transmission rate and improve the electrochemical behavior of thionine. Therefore, a wide linear range for the detection of TCA was estimated to be from 6  $\mu$ M to 1.5 mM with high sensitivity and good selectivity.

© 2010 Elsevier B.V. All rights reserved.

### 1. Introduction

Recently, metal-oxide nanotubes are emerging as potentially useful materials. The metal-oxide nanotubes are unique one-dimensional (1D) nanostructures with uniform nanometer-sized channels possessing electronic conductivity and high specific surface area. Therefore, they often play the role as the enhanced agents for effective acceleration of electron transfer between electrode matrix and target molecules. In addition, they are becoming a hot research topic especially in the construction of various architectures on the surface of electrodes due to their physical and chemical stability. Noticeably, TiO<sub>2</sub>-based nanotubes are of particular interest because of their potential applications as photocatalysts [1], sensors [2,3], electrochemical capacitors [4] and as lithium-inserting materials [5,6]. Among 1D TiO<sub>2</sub> nanostructures, titanate nanotubes (TNTs) have become one of the most powerful and promising material in various fields [7]. The multilayered and nanometer-scale inner-core cavity structures which are exposed to the outer surface [8], could provide a unique reaction vessel for analytes. It has been recently reported that the surface of the TNTs may easily be negatively charged after treatment with weak bases [9–12]. Furthermore, active groups, such as hydroxyls, on the nanotubes' surface may exhibit some kind of interaction with the analyte in the solution. These interesting properties of TNTs encourage us to investigate its possible sensing applications.

Till now, there are only a few reports about the electrochemical application of TNTs. Chen and co-worker [2] immobilized TNTs on glassy carbon electrode (GCE) to detect dopamine in the presence of a large amount of ascorbic acid and uric acid. Xiao et al. [13] investigated the electrochemical behavior of DA in the methylene blue/TNT layer-by-layer assembly multilayer films. However, up to the present, there is still no report about the immobilization of redox mediator onto the TNTs-based sensing interface. Thionine (TH), a cationic organic redox dye [14], is known to show a reversible process with good stability and reproducibility. As redox mediator, thionine has good conductivity for electron transfer and high electrochemical signal. Hence, it has been widely used in the fabrication of various biosensors, such as H<sub>2</sub>O<sub>2</sub> biosensor [15], electrochemical sensor for immunoassay of carcinoembryonic antigen [16] and NADH biosensor [17], etc.

Trichloroacetic acid (TCA), as an organohalide pollutant, is one of the major environmental concerns due to its extensive use in agriculture and public health programs [18]. Urinary TCA has been proposed as a biomarker of chronic ingestion exposure to non-volatile haloacetic acids from chlorinated drinking water [19,20]. Recently it has been urgently appealed by World Health Organization to develop rapid, reliable and accurate analytical methods for the detection of TCA [21]. Generally, the current methods for the detection of TCA are GC and HPLC [20,22,23]. Although these methods have adequate sensitivity, they suffered from expensive equipments, time-consuming for procedures of derivation and extraction and difficulty for in situ or online monitoring. In contrast to this, electrochemical sensors show its advantages over these drawbacks. Some electrochemical biosensors [24–26] and nano-

\* Corresponding author. Tel.: +86 591 87893315; fax: +86 591 83713866.  
E-mail address: [gnchen@fzu.edu.cn](mailto:gnchen@fzu.edu.cn) (G. Chen).

materials modified biosensors [27–29] have been developed for the detection of TCA. While, the sensitizing efficiency is limited, and the detection range is relatively narrow, also, the stability of immobilized proteins limits the practical application of these biosensors. Recently, Ju's group [30] fabricated a sensitive amperometric biosensor for trichloroacetic acid. The detection limit and the linear range was improved remarkably. However, to the best of our knowledge, till now there are still no paper reported using TH as electrochemical mediator for detection of TCA.

We used layer-by-layer technique to fabricate chitosan/TNTs/TH film modified electrochemical sensing platform. TNTs were firstly self-assembled on the chitosan (CHIT) membrane, which displays excellent film-forming ability, high permeability and susceptibility to chemical modifications. Then TNTs as the new type of catalysis material possessing some special physicochemical properties, is a kind of ideal support for different materials through high cation exchange and strong interaction with ion. Moreover, high specific surface area would lead to more material absorption. Therefore, TH as a model redox mediator, is then expected to strongly interact with the TNTs-based matrix. Based on this sensing platform, a cheap, rapid and sensitive electrochemical detection method for TCA was developed.

## 2. Experimental

### 2.1. Reagents

Chitosan of low molecular weight from the shrimp shell with a degree of deacetylation of 83.3% and thionine acetate were obtained from Sigma–Aldrich. TCA (>99%) was purchased from Shanghai Lingfeng Chemical Reagents Ltd. (China). All other chemicals were of analytical reagent grade and used without further purification. The 0.2 M acetate buffer solutions at various pH values were prepared by mixing the stock solutions of  $\text{CH}_3\text{COOH}$  and  $\text{CH}_3\text{COONa}$ . Ultrapure water from a Milli-Q plus system (Millipore

Co.,  $>18 \text{ MX cm}^{-1}$ ) was used in all aqueous solutions and rinsing procedures.

### 2.2. Apparatus

A model VMP3 Multichannel Potentiostats and Power Boosters (Princeton Applied Research, USA) was used for ac impedance measurement. Cyclic voltammetry (CV) scans were recorded using a CHI620 electrochemical workstation (CHI, USA) with a conventional three-electrode electrochemical cell using a glassy carbon (GC) electrode (4 mm diameter), KCl-saturated silver–silver chloride (Ag|AgCl) and a platinum wire as the working, reference and counter electrodes, respectively. All potentials reported here refer to the Ag|AgCl(sat. KCl) reference electrode. Transmission electron microscope (TEM) measurements were conducted by TECNAI G2F20 (FEI Company, The Netherlands). X-ray photoelectron spectroscopy (XPS) measurements were carried out with ESCALAB 250 A 1314.

### 2.3. Synthesis of TNT and preparation of TNT colloidal suspensions

TNTs were synthesized by a hydrothermal process based on a previously reported procedure [31]. A colloidal suspension of TNTs was prepared as follows: a suitable amount of TNTs powder was dispersed in a 0.1 M  $\text{HNO}_3$  solution under stirring and centrifugalization. The resulting deposit was further dispersed in 0.05 M tetraethylammonium hydroxide (TEAOH) while stirring, resulting in a translucent suspension solution. The as-prepared suspension was diluted with water and sonicated for another 5 min immediately before use.

### 2.4. Electrode preparation and modification

Before modification, the bare glassy carbon electrode was polished with 0.05  $\mu\text{m}$  alumina slurry, sonicated in deionized water,

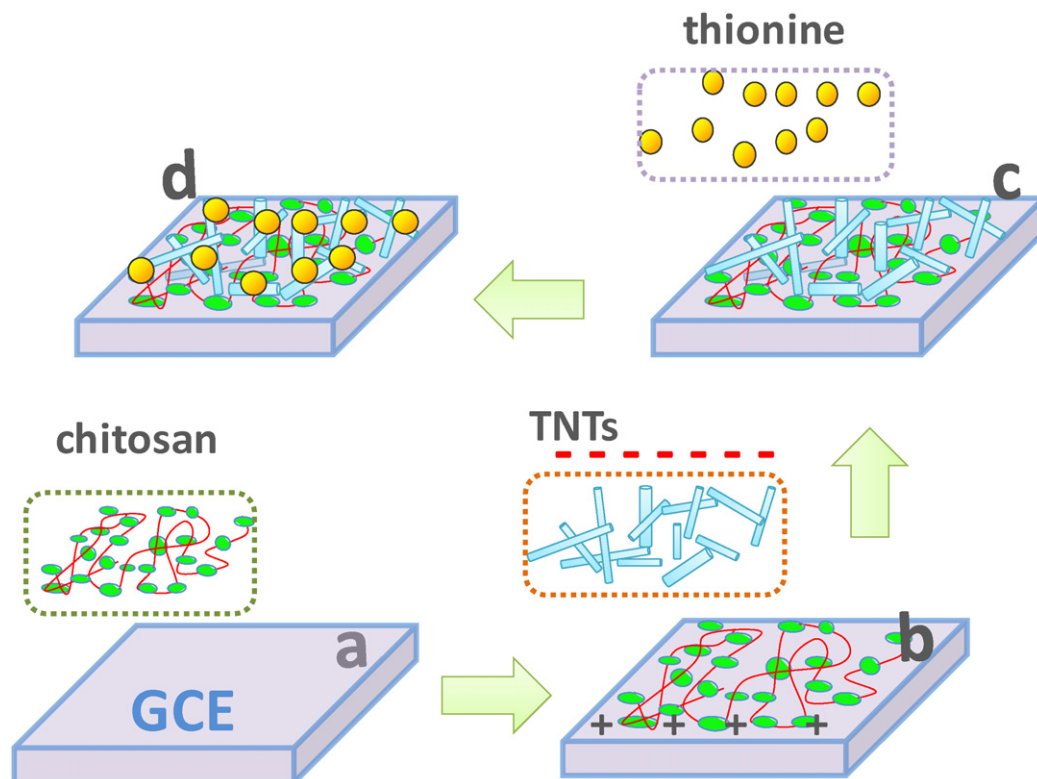


Fig. 1. A schematic showing the steps involved in the fabrication of the TH/TNTs/CS/GC electrode.

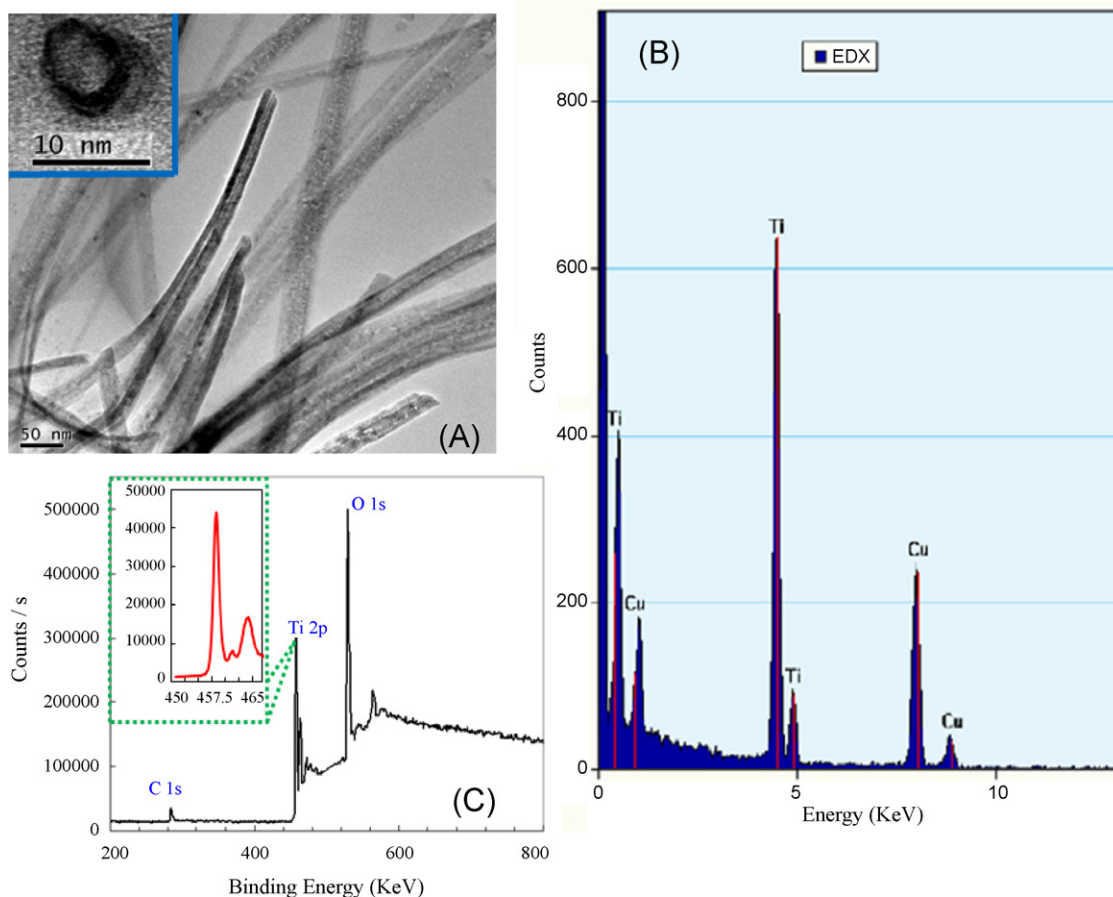


Fig. 2. TEM image of TNTs (A) and EDX spectrum of TNTs (B) and XPS spectra of TNTs (C).

and dried with high purify nitrogen stream to obtain a mirror surface. As shown in Fig. 1, a 10  $\mu\text{L}$  aliquot of 0.5 wt.% chitosan (CS) solution was then uniformly cast onto the GCE surface. The electrode was covered by a beaker and then dried under an infrared lamp. The CS modified GCE was immersed in negatively charged TNTs colloidal suspensions (2.5  $\text{mg mL}^{-1}$  of 0.05 M TEAOH solution). After being washed with water, the electrodes were then soaked in phosphate buffer (pH 7.0, 0.1 M) containing 0.3  $\text{mg mL}^{-1}$  thionine, where thionine had positive surface charges. To obtain good cyclic voltammetric responses of CS/TNT/TH GCE, the assembly time of TNTs and TH were optimized in control experiments. Typically, an assembling time of 25 min for TNTs and 20 min for TH was chosen.

### 3. Results and discussions

#### 3.1. Characterization of the prepared titanate nanotubes

TEM images (see Fig. 2A) convincingly revealed one-dimensional (1D) nanostructured materials of TNTs. It is clearly observed in Fig. 2 that the hollow nature of tubes with two ends open and the length up to micron. The insets in Fig. 2A indicated the nanotubes have open ends. Meanwhile, the EDX pattern in Fig. 2B indicated the titanium contained composite of the resultant substance. X-ray photoelectron spectroscopy (XPS) measurement was also performed to determine the chemical composition of the prepared TNTs and the valence states of various species. The obvious peaks mainly attributing to the Ti and O element appeared in the XPS survey spectra of pure TNTs (Fig. 2C). It can be known from the inset of Fig. 2C, the symmetric peaks of high-resolution XPS

spectra of Ti element located at 458.3 and 464.0 eV are attributed to the spin-orbit splitting of the Ti 2p components, which are in good agreement with the titanium(IV) species [32].

#### 3.2. Electrochemical behavior of various modified electrodes

The electrochemical behaviors of various modified electrodes were examined by cyclic voltammograms and ac impedance experiments in a buffer solution containing 5.0 mM  $\text{Fe}(\text{CN})_6^{3-}$  (see Fig. 3). It can be known from Fig. 3 that the peak current of CS/GCE is the highest, and the value was nearly four times greater than that of bare GCE, which might be due to the positive charge surface of CS film. Meanwhile the peak-to-peak separation became larger indicating CS might block the transfer of the electron through the film. However, after modifying the CS/GCE with TNTs, the peak currents decreased remarkably and became the smallest among the electrodes. It proved that TNTs carried stronger negative surface charge, after combining with positive CS molecules, the still TEM images (see Fig. 2A) convincingly revealed one dimensional (1D) nanostructured materials of TNTs negatively charged electrode surface played a crucial role in the diffusion of  $\text{Fe}(\text{CN})_6^{3-}$ . When finally assembled with TH, the peak current increased and was even bigger than that of bare GCE, also, the peak potential difference value became nearly the same as that of bare GCE. This was expected because the electrostatic attraction between  $\text{Fe}(\text{CN})_6^{3-}$  and the positively charged TH on the electrode surface facilitates  $\text{Fe}(\text{CN})_6^{3-}$  diffusion to the electrode surface. These evidences were also attained by ac impedance experiment shown in Fig. 3B. The Randles circuit (inset of Fig. 3) was chosen to fit the obtained impedance data. The resistance to charge transfer

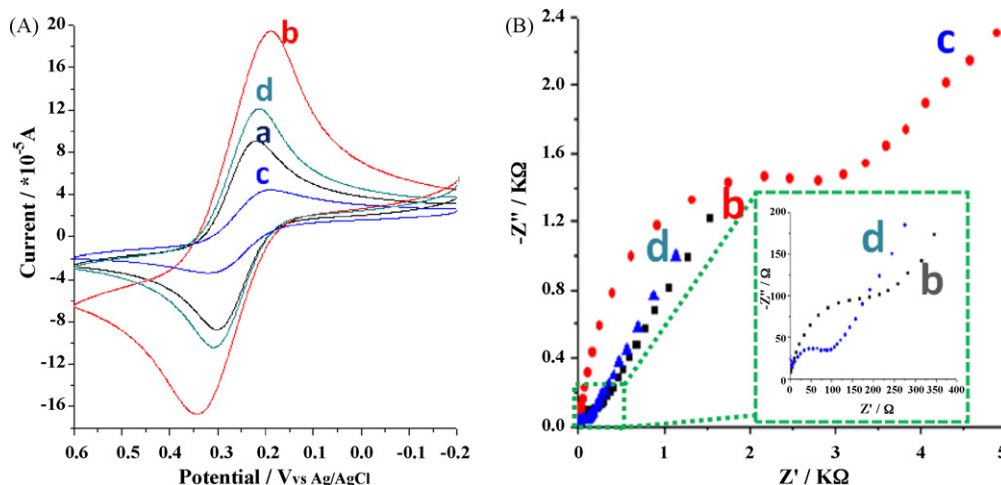


**Fig. 3.** Electrochemical behavior of various modified electrodes: (A) cyclic voltammograms at different modified glassy carbon electrodes. (B) Nyquist plots at various modified electrodes. (a) GCE; (b) CS/GCE; (c) TNTs/CS/GCE; (d) TH/TNTs/CS/GCE. Scan rate:  $50 \text{ mV s}^{-1}$ . Supporting electrolyte:  $5.0 \text{ mM Fe(CN)}_6^{3-}/\text{Fe(CN)}_6^{4-} + 0.5 \text{ M KCl}$ .

( $R_{ct}$ ) and the diffusion impedance ( $W$ ) were both in parallel to the interfacial capacitance ( $C_{dl}$ ). The diameter of the semicircle corresponded to the interfacial electron transfer resistance ( $R_{ct}$ ) [33]. By fitting the data,  $R_{ct}$  could be estimated to be  $170 \Omega$  at CS/GCE and increased to  $3.2 \times 10^3 \Omega$  at TNT/CS/GCE, suggesting that the TNT film blocked the diffusion of the ferricyanide anion to the electrode surface owing to the electrostatic force between TNTs and ferricyanide anion. While the value for TH/TNT/CS/GCE was decreased to  $78 \Omega$ , which revealed that the electron transfer resistance at TH/TNT/CS/GCE was much lower than those at CS/TNT/GCE and CS/GCE. This result suggested a decreased bulky resistance between  $\text{Fe(CN)}_6^{3-}$  and the TH/TNT/CS/GCE, which proved that TNTs carried a stronger negative surface charge and combined with positive TH molecules tightly and largely through the Coulomb force. Furthermore, it might indicate that TH/TNT/CS/GCE could provide a good electron pathway between the electrode and electrolyte and could accelerate the electron transfer rate from the film to the matrix of the electrode. Thus, the EIS analysis was consistent with the CV measurements.

Additionally, from the value of  $R_{ct}$  obtained by above ac impedance experiments, electron transfer rate constant ( $k^0$ ) can be calculated by Ref. [34]:

$$k^0 = \frac{RT}{F^2 R_{ct} A C} \quad (1)$$

where  $R$  is the gas constant,  $T$  the temperature,  $F$  the Faraday constant,  $A$  the geometric area and  $C$  the concentration of  $\text{Fe(CN)}_6^{3-}$ . For TH/TNT/CS/GCE,  $k^0$  was estimated as  $5.40 \times 10^{-3} \text{ cm s}^{-1}$ . On the basis of the results above, we summarized the important data in Table 1.

### 3.3. Electrochemical characteristics of adsorbed thionine

Cyclic voltammograms of CS/GCE and CS/TNT/GCE in acetate buffer did not show any observable peak (see Fig. 4, curve a and b), while CS/TNT/TH/GCE obviously exhibited a pair of distinct redox peaks (see Fig. 4, curve c) in the same potential range due to the redox of thionine adsorbed on the electrode surface at the

**Table 1**  
Summary of the important electrochemical data for various modified electrodes.

|               | $\Delta E$ (mV)    | $R_{ct}$ ( $\Omega$ ) | $k^0$ ( $\times 10^{-3}$ ) ( $\text{cm s}^{-1}$ ) |
|---------------|--------------------|-----------------------|---|
| CS/GCE        | $1.39 \times 10^2$ | $1.72 \times 10^2$    | $0.25 \times 10^1$                                |
| CS/TNT/GCE    | $1.30 \times 10^2$ | $3.20 \times 10^3$    | $1.30 \times 10^{-2}$                             |
| CS/TNT/TH/GCE | $0.85 \times 10^2$ | $0.78 \times 10^2$    | $0.54 \times 10^1$                                |

formal potential ( $E^0$ ) of ca.  $-0.12 \text{ V}$ . This result indicated that a large amount of thionine had been successfully incorporated into the CS/TNTs composite film by the combination with negatively charged TNTs through the Coulomb force. Moreover, the larger charge current of TNTs/CS/GCE than that case of CS/GCE just indicated that the rich functional hydroxyl groups on the inner-cavity surface and outer surface of TNTs probably provided a sort special reaction vessel for electrocatalytic action of analyte.

Fig. 5 showed the voltammograms of the CS/TNT/TH/GCE in  $0.20 \text{ M}$  acetate buffer solution at various potential scan rates in the range of  $30\text{--}120 \text{ mV s}^{-1}$ . The inset of Fig. 5A showed the linear relationship between the peak current and scan rate with a correlation coefficient of  $0.9930$ . The peak-to-peak separation also increased with the scan rate, which was characteristic of quasi-reversible surface controlled thin-layer electrochemical behavior. The integration of reduction peaks gave nearly constant charge ( $Q$ ) values at different scan rates. According to the following equation, the surface concentration ( $\Gamma^*$ ) of electroactive TH in the film was calculated

$$Q = nFA\Gamma^* \quad (2)$$

where  $Q$  is the charge passing through the electrode with full reduction of TH in the film,  $A$  is the geometric area of the modified GCE,  $n$  and  $F$  have their usual meaning, and  $\Gamma^*$  is the surface concentration of the electroactive substance. According to this method,

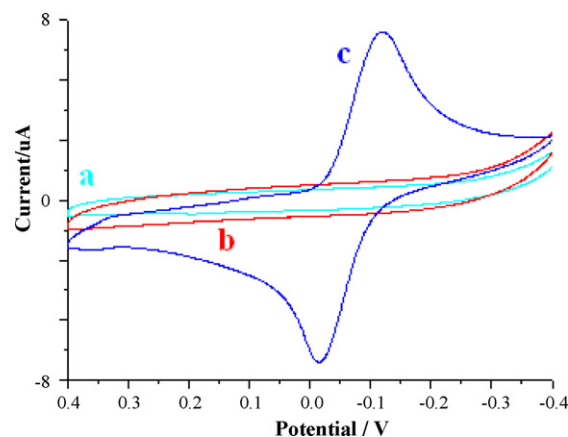


**Fig. 4.** Redox activity of the modified electrodes. (a) CS/GCE; (b) TNTs/CS/GCE; (c) TH/TNTs/CS/GCE. Scan rate:  $100 \text{ mV s}^{-1}$ . Supporting electrolyte:  $0.20 \text{ M}$  acetate buffer solution ( $\text{pH } 5.5$ ).



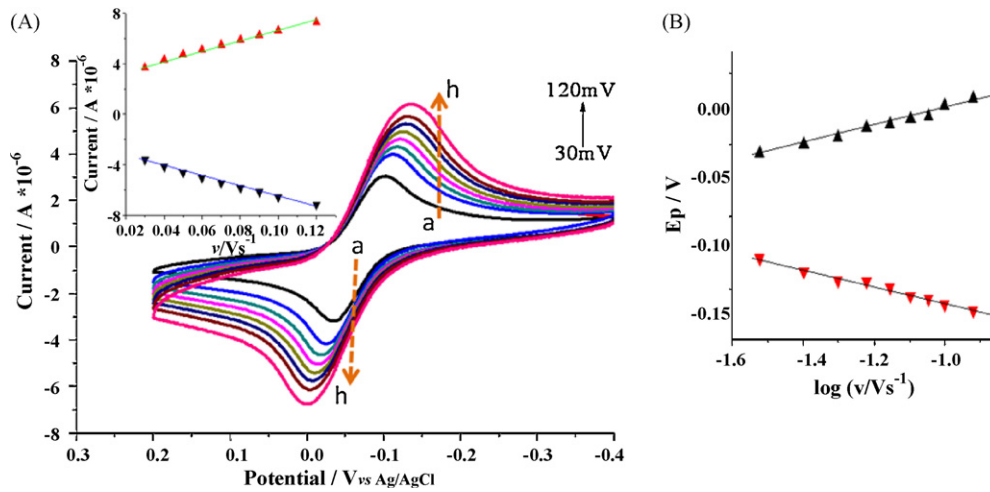


**Fig. 5.** (A) Redox activity of TH/TNTs/CS/GCE in 0.20 M acetate buffer solution (pH 4.5) versus different scan rate (from a to h: 0.03, 0.04, 0.05, 0.06, 0.07, 0.08, 0.09, 0.1, and 0.12  $V s^{-1}$ ). The inset shows the dependence of redox peak currents on the potential sweep rates. (B) The plot of anodic and cathodic peak potential of TH/TNTs/CS/GCE in 0.20 M acetate buffer solution (pH 4.5) with different scan rate.

the surface concentration of TH in the film ( $\Gamma^*$ ) was calculated as  $2.0 \times 10^{-10} \text{ mol cm}^{-2}$  by integration of the reduction peak in acetate buffer solution. The number of electrons involved in electron transfer reaction ( $n$ ) and the charge transfer coefficient ( $\alpha$ ) for TH/TNT/CS/GCE were estimated by cyclic voltammetry with Laviron's method [34] based on following equations:

$$E_{pc} = E^{o'} - \frac{2.3RT}{\alpha nF} \log v \quad (3)$$

$$E_{pa} = E^{o'} + \frac{2.3RT}{(1-\alpha)nF} \log v \quad (4)$$

where  $R$  is the charge transfer coefficient and  $F$  is the Faraday constant.

The relationships of peak potentials with  $\log v$  were shown in Fig. 5B. According to Eqs. (3) and (4), the charge transfer coefficient ( $\alpha$ ) and the number ( $n$ ) of transfer-electron can be calculated and the results found were 0.52 and 1.95, respectively, indicating that the electron transfer was a two-electron transfer.

#### 3.4. Analytical properties of TCA sensor

Electrochemical catalytic action of TCA towards TH was investigated by cyclic voltammetry (see Fig. 6). When TCA was added to a pH 5.5 acetate buffer, the TH redox peak of CS/TNT/TH film was observed remarkably increased, indicating the electrochemical catalytic action of TCA towards the electrochemical behavior of TH. Meanwhile, the more TCA that was added, the larger the redox peak current was achieved.

The previous reports indicated that the carboxyl group can interact with the surface of metal oxide [35–37]. We inferred the carboxylic group of TCA may interact with the TNTs, which leads to physical and chemical surface adsorption forms including the simple adsorption, hydrogen bonding and chemical binding. All these interaction were expected to the electron injection capability. Therefore, just due to the appearance of TCA, it results in the change of electrochemical behavior of TH. Hence, based on such experimental phenomena, the TH redox peak currents were linearly proportional to the concentration of TCA. Fig. 6 showed the linear dependence of the anode current on the TCA concentration. The linear regression equation was

$$I_{ac} (\times 10^{-6} \text{ A}) = 9.89 C (\times 10^{-3} \text{ mol L}^{-1}) + 2.012$$

in the range of  $1.5 \times 10^{-5}$  to  $1.5 \times 10^{-3} \text{ mol L}^{-1}$  with a correlation coefficient of 0.9980. The CS/TNT/TH electrode may be used to detect organohalide pollutants in the environment.

The stable cyclic voltammograms response of such TCA sensor for  $8.0 \times 10^{-5} \text{ mol L}^{-1}$  TCA could be achieved within 90 s after adding TCA. Different aspects regarding the characteristics of the CS/TNT/TH electrode were evaluated. The relative standard deviation (RSD) was 6.13% estimated from the response of six different and freshly prepared electrodes, revealing an acceptable repeatability in the construction of the sensor. Furthermore, such TCA sensor also exhibited good repeatability with relative standard deviations of 3.78% and 3.04% for eight determinations of  $8.0 \times 10^{-5} \text{ mol L}^{-1}$  and  $1.0 \times 10^{-3} \text{ mol L}^{-1}$  TCA.

When the resultant sensor was not in use, it was stored at room temperature. Electrode stability was tested daily over a 14 days period. It could maintain 89.3% of its initial electrochemical response after 2 weeks. This implied that the TNTs-based electrochemical platform is efficient for immobilizing the electrochemical

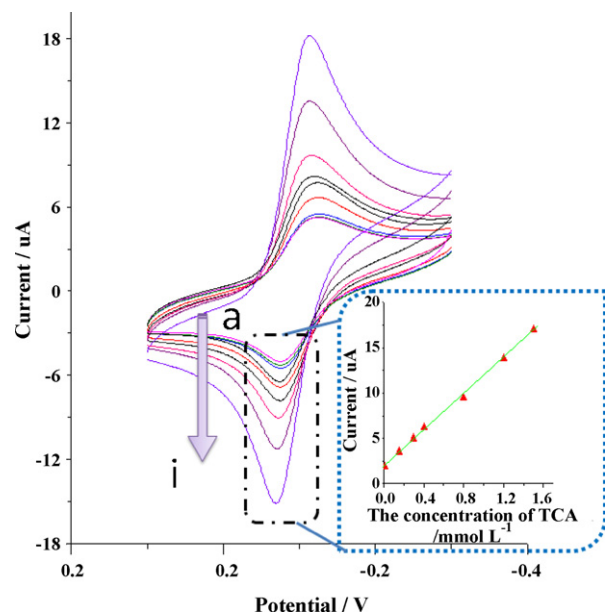


**Fig. 6.** Cyclic voltammograms of TH/TNTs/CS/GCE in 0.20 M acetate buffer solution (pH 5.5) with the increasing concentration of TCA (from a to i: 0, 0.006, 0.01, 0.15, 0.3, 0.4, 0.8, 1.2, and 1.5  $\text{mmol L}^{-1}$ ). Scan rate: 100  $\text{mV s}^{-1}$ .

probe and preventing the leak of electrochemical probe from the sensor.

It is envisaged that the practical usefulness of a sensor often rests upon the selectivity and its anti-interference property. So the determination of TCA in the presence of coexisting ions and other compounds was also studied. A foreign species was considered not to interfere if it caused a relative error <10% for the measurement of  $5.0 \times 10^{-4}$  M TCA. The results illustrated that the tolerated ratio of foreign substances to  $5.0 \times 10^{-4}$  M TCA was 800-fold for  $\text{Na}^+$ ,  $\text{K}^+$ ,  $\text{Mg}^{2+}$ ,  $\text{Al}^{3+}$ ,  $\text{NH}_4^+$ ,  $\text{SO}_4^{2-}$ ,  $\text{PO}_4^{3-}$ ,  $\text{Cl}^-$  and  $\text{NO}_3^-$ ; 100-fold for ethanol, methanol, sucrose and glucose.

#### 4. Conclusions

A new TNTs contained electrochemical sensing platform for TCA based on the TCA electrocatalytic action towards TH was first reported. The TNTs adopted in the fabrication of proposed sensor could play the crucial role as follows: high ratios of surface area to volume and the strong negative charged surface of TNTs could result in the effective and firm immobilization of redox mediator onto the sensing interface. And TNTs would effectively enhance the electron transfer between matrix and redox mediator. Benefiting from the proposed properties of TNTs, the electrochemical investigation demonstrated that the model redox mediator, TH, kept quite sensitive and stable electrochemical action. TCA was showed highly electrocatalytic response towards the redox of TH, dramatically amplifying the redox electrochemical response of TH. A wide linear range for the detection of TCA was estimated to be from  $15 \mu\text{M}$  to  $1.5 \text{ mM}$  with high sensitivity and good selectivity. Therefore, the TNTs containing sensing platform for the immobilization of cation redox mediator has excellent prospects for designing a new bioelectronic devices with high sensitivity.

#### Acknowledgements

This project was financially supported by National Basic Research Program of China (No. 2010CB732403), the NSFC (20735002, 20877019), the Science and Technology Development Funding of Fuzhou University (826249) and program for New Century Excellent Talents in University (NECT-06-0572) of China and Fujian province.

#### References

- [1] M. Adachi, Y. Murata, M. Harada, S. Yoshikawa, *Chem. Lett.* 16 (2000) 942.
- [2] S. Liu, A. Chen, *Langmuir* 21 (2005) 8409.
- [3] O.K. Varghese, D. Gong, M. Paulose, K.G. Ong, E.C. Dickey, C.A. Grimes, *Adv. Mater.* 15 (2003) 624.
- [4] Y.G. Wang, X.G. Zhang, *J. Electrochem. Soc.* 152 (2005) 671.
- [5] G. Armstrong, A.R. Armstrong, J. Canales, P.G. Bruce, *Chem. Commun.* 19 (2005) 2454.
- [6] H. Zhang, G.R. Li, L.P. An, T.Y. Yan, X.P. Gao, H.Y. Zhu, *J. Phys. Chem. C* 111 (2007) 6143.
- [7] D.V. Bavykin, J.M. Friedrich, F.C. Walsh, *Adv. Mater.* 18 (2006) 2807.
- [8] Q. Chen, W. Zhou, Q. Chen, G. Du, L. Peng, *Adv. Mater.* 14 (2002) 1208.
- [9] R. Ma, Y. Bando, T. Sasaki, *Chem. Phys. Lett.* 380 (2003) 577.
- [10] R. Ma, Y. Bando, T. Sasaki, *J. Phys. Chem. B* 108 (2004) 2115.
- [11] Z.R. Tian, J.A. Voigt, J. Liu, B. McKenzie, H. Xu, *J. Am. Chem. Soc.* 125 (2003) 12384.
- [12] B.D. Yao, Y.F. Chan, X.Y. Zhang, W.F. Zhang, Z.Y. Yang, A. Liu, *Adv. Funct. Mater.* 16 (2006) 371.
- [13] M.W. Xiao, L. Wang, Y.D. Wu, *J. Solid State Electrochem.* 12 (2008) 1159.
- [14] K. Zhao, H.Y. Song, S.Q. Zhuang, L.M. Dai, P.G. He, Y.Z. Fang, *Electrochem. Commun.* 9 (2007) 65.
- [15] R. Yang, C.M. Ruan, W.L. Dai, J.Q. Deng, J.L. Kong, *Electrochim. Acta* 44 (1999) 1585.
- [16] Z. Dai, J. Chen, F. Yang, H.X. Ju, *Cancer Detect. Prev.* 29 (2005) 233.
- [17] Q. Gao, X.Q. Cui, F. Yang, Y. Ma, X.R. Yang, *Biosens. Bioelectron.* 19 (2003) 277.
- [18] J.N. Cape, S.T. Forczek, G. Gullner, G.M. Benitez, P. Schroder, M. Matucha, *Environ. Sci. Pollut. Res.* 13 (2006) 276.
- [19] World Health Organization Guidelines for Drinking Water Quality, vol. 2, Health.
- [20] J.W. Miller, P.C. Uden, R.M. Barnes, *Anal. Chem.* 54 (1982) 485.
- [21] Y.H. Wang, P.K. Wong, *Water Res.* 39 (2005) 1844.
- [22] D.O. Johns, R.L. Dills, M.S. Morgan, *J. Chromatogr. B* 817 (2005) 255.
- [23] Z. Kuklennyik, D.L. Ashley, A.M. Calafat, *Anal. Chem.* 74 (2002) 2058.
- [24] Y.L. Zhou, Z. Li, N.F. Hu, Y.H. Zeng, J.F. Rusling, *Langmuir* 18 (2002) 8573.
- [25] H.Y. Ma, N.F. Hu, J.F. Rusling, *Langmuir* 16 (2000) 4969.
- [26] W. Sun, R.F. Gao, K. Jiao, *J. Phys. Chem. B* 111 (2007) 4560.
- [27] Y.C. Li, W.W. Yang, Y. Bai, C.Q. Sun, *Electroanalysis* 18 (2006) 499.
- [28] Y.H. Zhang, X. Chen, W.S. Yang, *Sens. Actuator B: Chem.* 130 (2008) 682.
- [29] Y. Liu, X. Qu, H. Guo, H. Chen, B. Liu, S. Dong, *Biosens. Bioelectron.* 21 (2006) 2195.
- [30] W. Tu, J. Lei, H. Ju, *Chem. Eur. J.* 15 (2009) 779.
- [31] T. Kasuga, M. Hiramatsu, A. Hoson, T. Sekino, K. Niihara, *Langmuir* 14 (1998) 3160.
- [32] P. Wauthoz, M. Ruwet, T. Machej, P. Grange, *Appl. Catal.* 69 (1991) 149.
- [33] A.J. Bard, L.R. Faulkner, *Electrochemical Methods: Fundamentals and Applications*, John Wiley & Sons, New York, 2001, p. 380.
- [34] E. Laviron, *J. Electroanal. Chem.* 100 (1979) 263.
- [35] P.A. Connor, K.D. Dobson, A.J. McQuillan, *Langmuir* 11 (1995) 4193.
- [36] K. Murakoshi, G. Kano, Y. Wada, *J. Electroanal. Chem.* 396 (1995) 27.
- [37] Y.X. Weng, L. Li, Y. Liu, L. Wang, G.Z. Yang, *J. Phys. Chem. B* 107 (2003) 4356.